Interaction Notes
Note 579
10 February 2003

A Quantitative Comparison between the Matrix Pencil Method and the State Space Based Harmonic Retrieval Methods

Seongman Jang, Wonsuk Choi and Tapan K. Sarkar
Department of Electrical Engineering and Computer Science
Syracuse University, 121 Link Hall, Syracuse, NY 13244

Abstract-The approximation of a function by a sum of complex exponentials is treated here. In particular, the Matrix Pencil Method and the state space based harmonic retrieval methods are compared quantitatively. It is known that the two methods generate very similar results when there is no noise in the data and have only minor differences between them, when the data is contaminated by noise. But quantitative comparison between them has not been reported so far. In this paper, their comparison is done with respect to the determination of the poles from transient impulse response of various electromagnetic systems.

This work was supported in part by the Air Force Research Laboratory, Directed Energy Directorate, Kirtland Air Force Base, New Mexico.

1. Introduction

In this paper two methods for approximating a real time domain signal with a minimum number of damped sinusoids are compared quantitatively. Usually, late time electromagnetic scattered field can be represented with damped sinusoids, which can be described by

$$\begin{aligned} y_k &= x_k + n_k \\ &= \sum\nolimits_{m=1\cdots M} |c_m| \exp[(\alpha_m + j\omega_m)k + j\phi_m] + n_k \end{aligned} \tag{1}$$

$k = 0, 1, \cdots, N-1$. n_k is the noise sequence. $|c_m|$ and ϕ_m are the amplitude and the phases, respectively. α_m and ω_m are the damping factors and the frequencies, respectively. M is the number of exponentials. We also write

$$R_m = |c_m| \exp(j\phi_m) \tag{2}$$

$$z_m = \exp(-\alpha_m + j\omega_m) \tag{3}$$

Since we are approximating the entire time domain transient response (i.e. both early and late time) using the superimposed damped sinusoids, the complex resonant pole, represented by the Equation (3) can be different from an analytic one. We are just interested in the minimum order of the approximation in terms of accuracy and running time, in this paper.

It is well known that the matrix pencil method and the state space approach generate very similar result for the exact data case and have minor differences for the noisy data case [2]. And also it is known that these two methods are equivalent to a first order approximation [1]. Both methods use the property of a Hankel matrix and singular value decomposition. The properties of the Hankel matrix play an important role in many occasions. The most significant role of the Hankel matrix is that the rank of the matrix for the ideal case will reflect the order of the corresponding system. And the number of nonzero singular values corresponds to the rank of the matrix. So, the set of singular values will be used to determine the rank as well as to judge the deviation of the matrix from a lower rank one [3].

Many kinds of Matrix Pencil Method and State Space Approach have been proposed. But in this study one Matrix Pencil method and two State Space approaches have been chosen that deal with approximating the time domain impulse response of a sequence, which corresponds

to the Markov parameters in the State space approach. The Total Least Square Matrix Pencil Method (TLS-MPM) [4] is chosen for the Matrix Pencil Method. The normal state space approach using singular value decomposition [3] is the first method and the state space approach using Extended Impulse Response Gramian [5] is the second method for the State Space approach.

We shall discuss those three methods briefly, and explain how to obtain the time domain impulse response sequence. Then several examples will be shown to compare the accuracy and execution time.

2. Total Least Square Matrix Pencil Method (TLS-MPM) [4]

The TLS-MPM approach is an efficient and robust method to fit noisy data with a sum of complex exponentials. [8][9] To implement TLS-MPM, one forms the data matrix [Y] using the input data y as

$$[Y]=\begin{bmatrix} y(0) & y(1) & \cdots & y(L) \\ y(1) & y(2) & \cdots & y(L+1) \\ \vdots & \vdots & & \vdots \\ y(N-L-1) & y(N-L) & \cdots & y(N-1) \end{bmatrix}_{(N-L)\times(L+1)} \tag{4}$$

where N is number of data and L is pencil parameter. For efficient noise filtering L is chosen N/3 to N/2. Then singular value decomposition (SVD) of the matrix [Y] is calculated as

$$[Y]=[U][\Sigma][V^H]. \tag{5}$$

Here, [U] and [V] are unitary matrices, composed of the eigenvectors of $[Y][Y]^H$ and $[Y]^H[Y]$, respectively, and [Σ] is a diagonal matrix containing the singular values of [Y]. At this stage, the number of exponentials is determined by the ratio of the singular values to the largest one. Consider the singular value σ_c such that

$$\frac{\sigma_c}{\sigma_{\max}} \approx 10^{-p}, \tag{6}$$

where p is the number of significant decimal digit in the data. For example, if the data is accurate up to 3 significant digits, then the singular values for which the ratio in the above equation is below 10^{-3} are essentially noise singular values, and they should not be used.

Next, consider the 'filtered' matrix, $[V']$, constructed so that it contains only M dominant right singular vectors of [V],

$$[V'] = [v_1, v_2, \cdots, v_m]. \tag{7}$$

The right singular vectors from M+1 to L, corresponding to the small singular values, are discarded. Therefore,

$$[Y_1] = [U][\Sigma'][V_1']^H, \tag{8}$$

$$[Y_2] = [U][\Sigma'][V_2']^H, \tag{9}$$

where $[V_1']$ is obtained from $[V']$ with the last row of $[V']$ deleted, $[V_2']$ is obtained by removing the first row of $[V']$, and $[\Sigma']$ is obtained from the M columns of $[\Sigma]$ corresponding to the M dominant singular values. The poles of the signals are given by the non-zero eigenvalues of

$$\left\{[V_1']^H\right\}^+ [V_2']^H \tag{10}$$

which are the same as the eigenvalues of

$$[V_2']^H \left\{[V_1']^H\right\}^+ \tag{11}$$

Once M and the poles ($z_i = \exp(-\alpha + j\omega)T_s$) are known, the residues, R_i, are solved from the following least square problem,

$$\begin{bmatrix} y(0) \\ y(1) \\ \vdots \\ y(N-1) \end{bmatrix} = \begin{bmatrix} 1 & 1 & \cdots & 1 \\ z_1 & z_2 & \cdots & z_M \\ \vdots & \vdots & & \vdots \\ z_1^{N-1} & z_2^{N-1} & \cdots & z_M^{N-1} \end{bmatrix} \begin{bmatrix} R_1 \\ R_2 \\ \vdots \\ R_M \end{bmatrix} \tag{12}$$

3. State Space Approach 1 [3]

Consider a stable, linear, time-invariant, discrete-time system of degree n described by the following minimal realization

$$\begin{aligned} x(k+1) &= Ax(k) + Bu(k) \\ y(k) &= Cx(k) \end{aligned} \tag{13}$$

In addition, $M_q(k,l)$ is a Hankel matrix and is defined by

$$M_q(k,l) = \begin{bmatrix} h(q) & h(q+1) & \cdots & h(l) \\ h(q+1) & h(q+2) & \cdots & h(l+1) \\ \vdots & \vdots & & \vdots \\ h(k) & h(k+1) & \cdots & h(k+l-q) \end{bmatrix} \tag{14}$$

where $h(k) = CA^{k-1}B$ = Markov parameters or impulse response sequence (15)

Given a minimal realization $\{A, B, C\}$ of degree n and $N \geq l$,the r^{th} order reduced model is obtained by the following procedure;

First, make the Hankel matrix $M_1(N+1, N+1)$ to be square, and then write the SVD of the Hankel matrix as

$$M = U\Sigma V^T \tag{16}$$

where $\Sigma = Diag\left[s(1), s(2), \cdots s(r), e(r+1), \cdots, e(n+N+1)\right]$,

with $s(1) \geq s(2) \geq \cdots s(r) \geq e(r+1) \cdots e(n+N+1)$

If the matrix $M_1(N+1, N+1)$ has a rank r then all the singular values e(i) should be zero. When the singular values e(i) are not zero but small, then one can easily recognize that the matrix is not too far away from a matrix of rank r. So, rearrange the matrix such that

$$M = U\Sigma V^T = \overline{U}\overline{V} \tag{17}$$

where $\overline{U} = U\Sigma^{1/2}$ *and* $\overline{V} = \Sigma^{1/2}V$.

Now the state space matrices A_r, B_r and C_r of the reduced system can be obtained from followings:

$$A_r = \overline{U}_1^{+}\,\overline{U}_2 \text{ or } A_r = \overline{V}_1\overline{V}_2^{+} \tag{18}$$

where + denotes the pseudoinverse and define

$\overline{U}_1$: the first N block rows and the first r columns of $\overline{U}$

$\overline{U}_2$: the last N block rows and the first r columns of $\overline{U}$

$\overline{V}_1$: the first r rows and the first N block columns of $\overline{V}$

$\overline{V}_2$: the first r rows and the last N block columns of $\overline{V}$

B_r, the input matrix of the reduced system is

$$B_r = \overline{V}^{(1)} \tag{19}$$

and the output matrix for the reduced system, C_r is

$$C_r = \overline{U}^{(1)} \tag{20}$$

where

$\overline{U}^{(i)}$: the i-th block row and the first r columns of $\overline{U}$

$\overline{V}^{(i)}$: the first r rows and the i-th block column of $\overline{V}$

Using these state space matrices, we can generate an impulse response of the reduced system and the system transfer function. Impulse response of the reduced system is given by

$$h(k) = CA^{k-1}B \tag{21}$$

And the transfer function of the reduced system is

$$H(z) = C_r[zI - A_r]^{-1}B_r \tag{22}$$

Now we can get the poles (P_{Ti}) of the reduced system using the state matrix, A_r as

$$P_{Ti} = \text{eigenvalue of } A_r$$

These poles will be discrete in z-domain, but we want to have them in the s-domain(P_i). We can find the poles in s-domain using

$$P_{Ti} = e^{P_i T} \quad _i = 1, 2, \ldots, n \tag{23}$$

where T is the sampling period. This completes the first state space method.

4. State Space Approach 2 with Extended Impulse Response Gramian (EIRG) [5]

Consider a stable, linear, time-invariant, discrete-time, multiple-input and multiple- output (MIMO) system of degree n described by the following minimal realization

$$\begin{aligned} x(k+1) &= Ax(k) + Bu(k) \\ y(k) &= Cx(k) \end{aligned} \tag{24}$$

The extended impulse response Gramian P_N of order N, for the system of degree n, is defined $\forall N \in Z^+ , N \geq n$ as the following

$$P_N = \sum_{k=0}^{\infty} \begin{bmatrix} H_{k+1}^T H_{k+1} & H_{k+1}^T H_{k+2} & \cdots & H_{k+1}^T H_{k+N} \\ H_{k+2}^T H_{k+1} & H_{k+2}^T H_{k+2} & \cdots & H_{k+2}^T H_{k+N} \\ \vdots & \vdots & \vdots & \vdots \\ H_{k+N}^T H_{k+1} & H_{k+N}^T H_{k+2} & \cdots & H_{k+N}^T H_{k+N} \end{bmatrix} \tag{25}$$

where

$$H_k = CA^{k-1}B = \text{ Markov parameters or impulse response sequence} \tag{26}$$

We write the SVD of the Extended Impulse Response Gramian as

$$P = U\Sigma V^T \tag{27}$$

where $\Sigma = Diag[s(1),\ s(2),\ \cdots,\ s(r),\ e(r+1),\ \cdots,\ e(n+N+1)]$; with

$s(1) \geq s(2) \geq \cdots s(r) \geq e(r+1) \cdots e(n+N+1)$.

If Gramian has a rank r then all the singular values e(i) should be zero. When the singular values e(i) are not zero but small, then one can easily recognize that the matrix is not too far away from a matrix of rank r.

And we define

$$\begin{aligned} X &\equiv (U\Sigma^{1/4})^T = \Sigma^{1/4}U^T \\ X_1 &\equiv [X^{<1>}\ X^{<2>} \cdots X^{<r+N>}] \\ X_2 &\equiv [X^{<2>}\ X^{<3>} \cdots X^{<r+N+1>}] \end{aligned} \tag{28}$$

where $M^{<j>} \equiv j$ th column block of matrix M truncated to first r elements

Now one can find the state space matrices A_r, B_r and C_r of the reduced system. State matrix of the reduced system, A_r is

$$A_r X_1 = X_2$$
$$A_r = X_2 X_1^+ \tag{29}$$

where + denotes a pseudoinverse. The input matrix of the reduced system, B_r is given by

$$B_r = X^{<1>} \tag{30}$$

And output matrix of reduced system, C_r is

$$\tilde{C} = HU\Sigma^{-1/4} \tag{31}$$

$$C_r = \tilde{C}^{((1))} \tag{32}$$

where $M^{((i))} \equiv i$ th row block of matrix M truncated to first r elements. If the state space matrices A_r, B_r and C_r are known the poles can be extracted using the same procedure as outlined for the previous approach.

5. Computation of the poles for a transient scattered field

In this study the transient electromagnetic scattered field is used as an impulse response sequence. To obtain the scattered field in the time domain, first, each example is analyzed in the frequency domain. Then the time domain data is calculated using the inverse Fourier transform of the frequency domain result. The backward scattered field is calculated using WIPL-D [10] in the frequency domain, which uses an electric field integral equation (EFIE) for the conducting structure and PMCHW for the composite structures. Before taking the inverse Fourier transform, a Gaussian window is applied to limit the bandwidth and make a smooth transition to the high frequency. The advantages of the Gaussian window are that it provides a smooth roll off in time and frequency and is well suited for numerical computation. The Gaussian window used to window the frequency domain data can be defined as Equation 25 and 26, [11]

$$g(t) = \frac{1}{\sigma\sqrt{\pi}} e^{-\gamma^2}, \tag{33}$$

with

$$\gamma = \frac{(ct - ct_0)}{\sigma}, \tag{34}$$

where c is the velocity of light, t_0 is a time delay which represents the peak time shifted from the origin, and σ is the pulse width which can be defined such that the peak value is fallen down to about 2% at t for $ct - ct_0 = \pm 2\sigma$. Figure 1 (a) shows an example of the temporal Gaussian pulse, where $\sigma = 1.0 lm$, and $ct_0 = 6.0 lm$ (The unit lm denotes a light meter. A light meter is the length of time taken by the electromagnetic wave to travel 1 m. Assuming the medium to be free space this amounts to 1 lm = 3.33564 ns). The Fourier transform of this pulse is

$$G(f) = \frac{1}{c} e^{-\left(\frac{\pi\sigma f}{c}\right)^2} e^{-j2\pi f t_0}, \tag{35}$$

and the frequency band corresponding to the pulse width is plotted in Figure1 (b). A wide band frequency results from a narrower pulse width in the time domain and vice versa.

6. Examples

6.1 Wire: The first example is a thin wire scattering element of length L and diameter d, which is excited by an incident pulse of electromagnetic radiation. The length of the wire scatterer is 50mm and the aspect ratio (L/d) is100. The incident field is coming from 45 degree from the wire axis and is polarized with respect to the theta direction

The normalized backward scattered field is obtained using WIPL-D [30], in the frequency domain. The frequency range covered is 0.2~100 GHz. A Gaussian window is applied to limit the maximum frequency. The parameters of the Gaussian window are $\sigma = 0.0035$ and $ct_0 = 14\sigma$. The time domain response due to the backward scattered field is obtained using the inverse Fourier transform (FFT) of the Gaussian windowed frequency domain data, which is shown in Figure 3. When taking the inverse Fourier transform some zeros are padded into the

frequency domain data to increase the resolution in the time domain. The sampling frequency of the resulting time domain data is 4 times that of the highest frequency of interest.

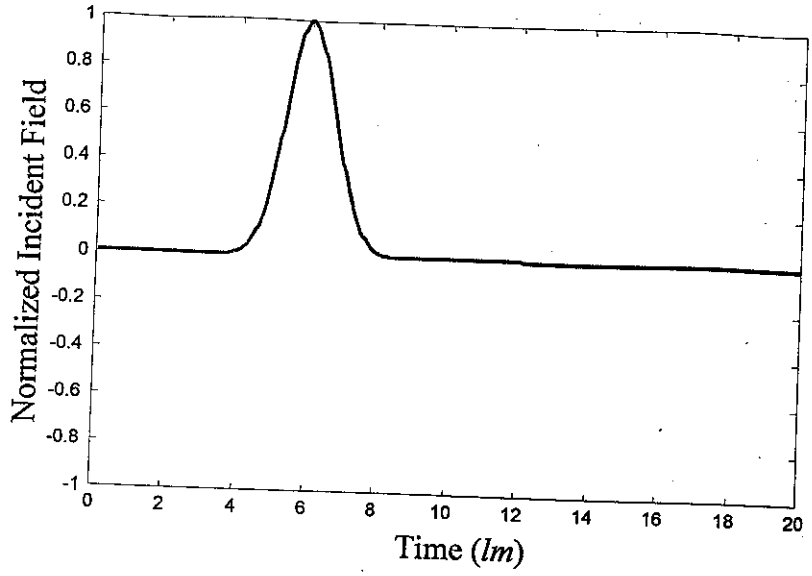

(a)

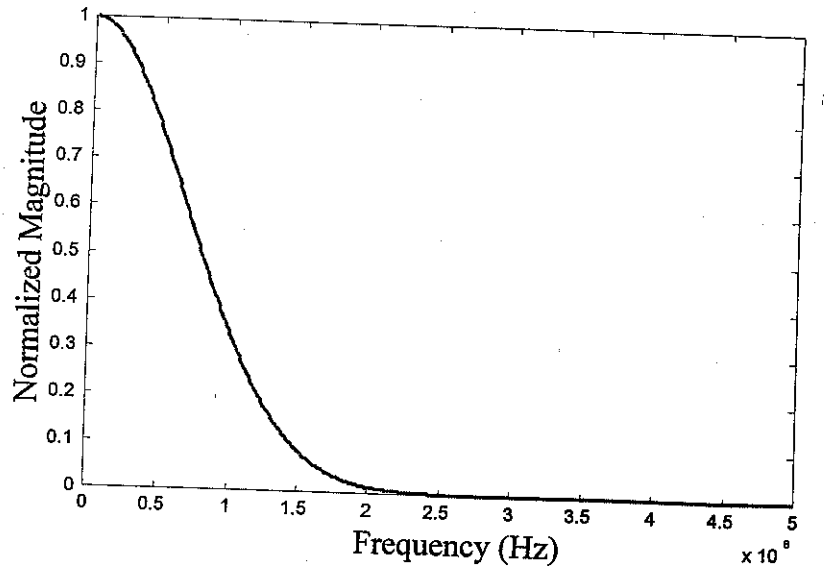

(b)

Figure 1. Plots of a Gaussian incident field in the (a) time domain and (b) its spectrum which is used for excitation.

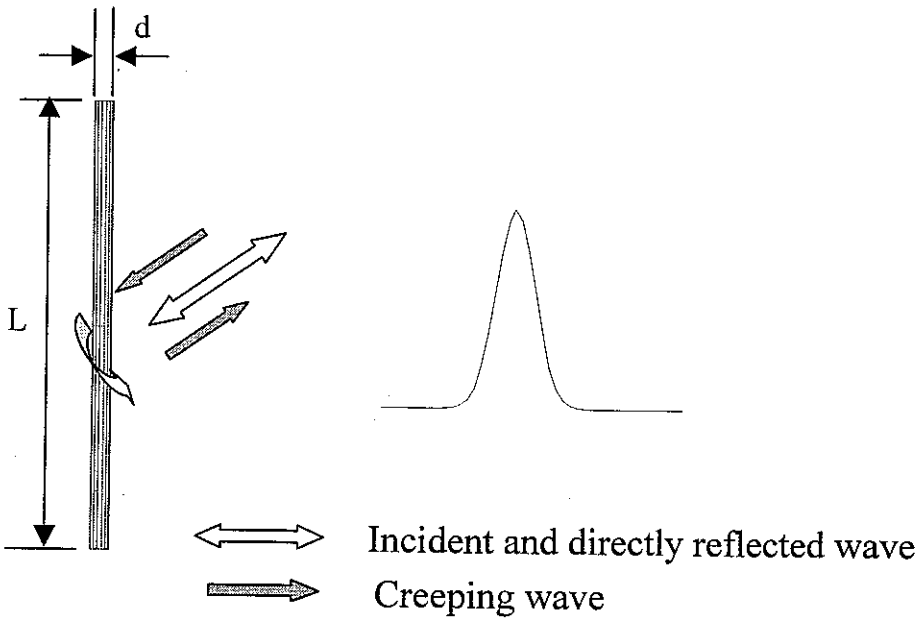

Figure 2. A wire scatterer model with a wave incident from $\theta = 45°$.

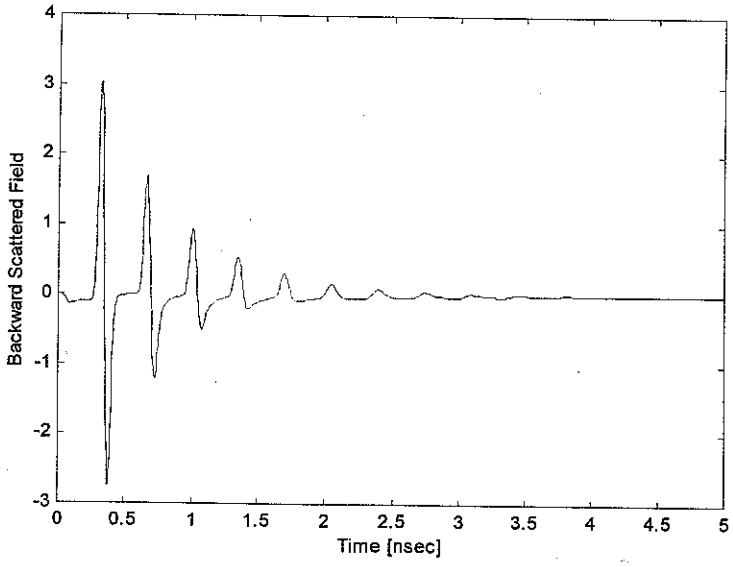

Figure 3. Backward scattered field in the time domain for a wire scatterer.

The target signal is real valued so one has a complex conjugate pole pair, which corresponds to two singular values, and constitutes one damped sinusoid. The test have been done with a fixed number of damped sinusoids so that the number of singular values which are two times the number of damped sinusoids are chosen and the corresponding poles are extracted. After calculating those poles the time domain signal is reconstructed using those poles and appropriate residues in the Matrix Pencil Method or using the zeros in the State Space method. The root mean square (RMS) error between the original signal and reconstructed signal is also computed. Figure 4 shows that the RMS error decreases with the number of damped sinusoids. One damped sinusoid is thus composed of one complex conjugate pole pair so that it uses two singular values. Circles represent the results from the matrix pencil method, the asterisks are the results for the first state space method (This is represented using 'SS1' in the legend) and the triangles are the results for the second state space approach (This is represented using 'SS2' in the legend). The unit of the Error axis is dB in scale and the threshold is set to -80 dB. It shows that RMS error between both the MPM and SS1 are the same when the error goes below the threshold and the transient response is approximated with 19 damped sinusoids. The error, however, for the SS2 decreases slowly and it requires 44 damped sinusoids to approximate the transient response before it goes below the threshold.

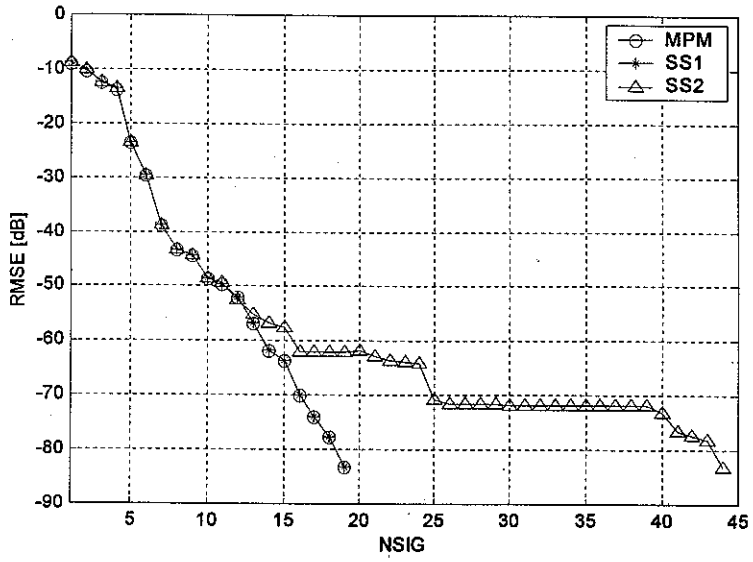

Figure 4. The RMS error in the reconstructed signal for a wire scatterer.

Figure 5 represent the CPU time taken by each method. The tests have been carried out in a same PC – (Intel Pentium IV, 2.4GHz, 2GB RAM). Average CPU time for the MPM is 11.4489sec, that for the SS1 is 16.8239sec and that for SS2 is 224.8235sec. CPU time for MPM is just 68% of that for SS1 and 5% of that for SS2.

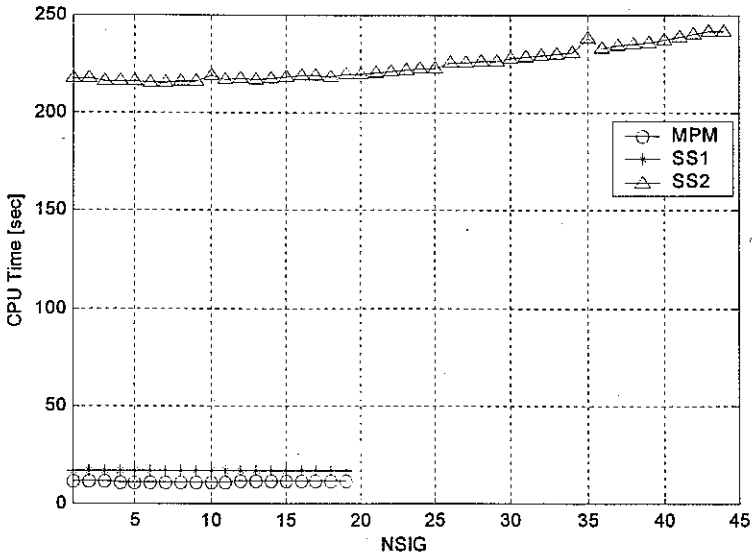

Figure 5. CPU time taken at each step for the analysis of the wire scatterer.

Figure 6 and 7 show the pole plot for NSIG = 10 and 15 respectively. NSIG represent the number of damped sinusoids. Just the node locations in the second quadrant are shown because of the symmetry of the complex poles. For NSIG = 10, all poles are same for the three methods but for NSIG = 15 case the location of the poles for the SS2 method differs from the other two methods.

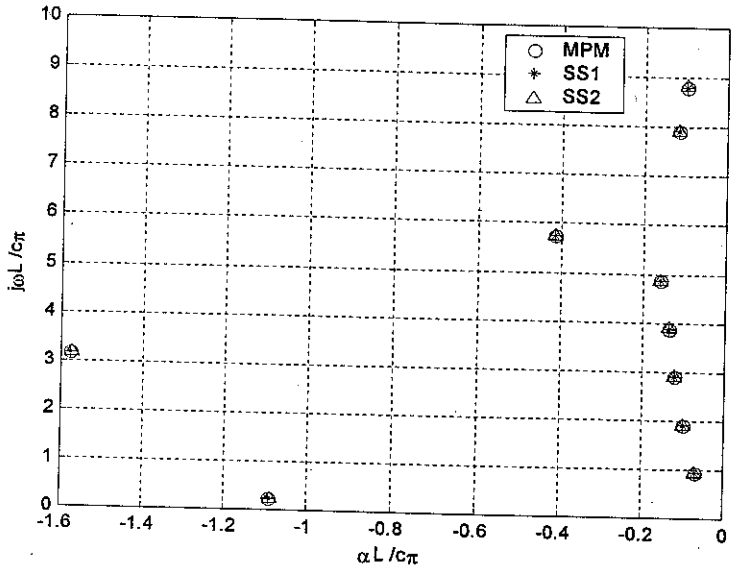

Figure 6. Extracted poles for NSIG = 10 of a wire.

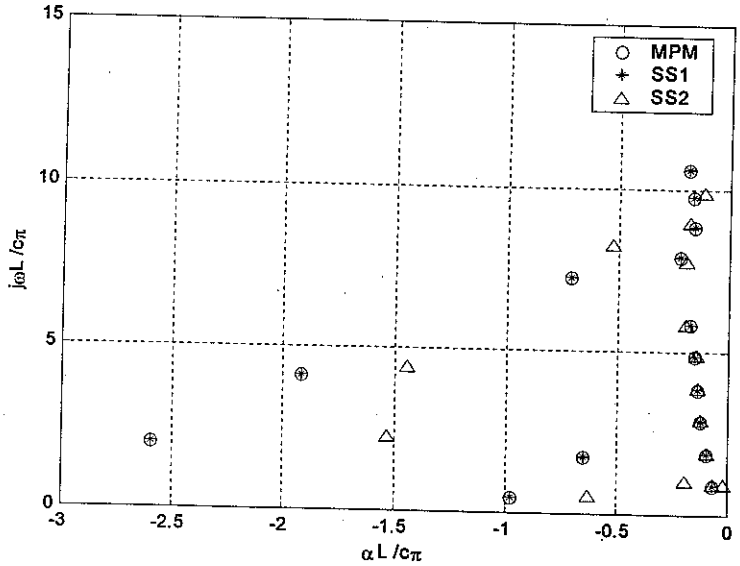

Figure 7. Extracted pole for NSIG = 15 of a wire.

6.2 Sphere

For the second example we consider a conducting sphere of radius 1cm, which is shown in Figure 8. The backward scattered field has been obtained using WIPL-D in the frequency

domain. The incident field is coming from the side and is z-polarized. A Gaussian window is applied to limit the bandwidth. The inverse transformed time domain data is shown in Figure 9. This data exhibits two kinds of pulses. One is a directly reflected pulse and another is a creeping wave. The time difference, in the location of those two pulses is about 0.176nsec. This shows a good agreement with the calculated value of 0.1714nsec. $\{(2+\pi)\,\mathrm{x}\,\mathrm{r}/3\mathrm{x}10^{8} = 0.1714\ \mathrm{nsec}\}$.

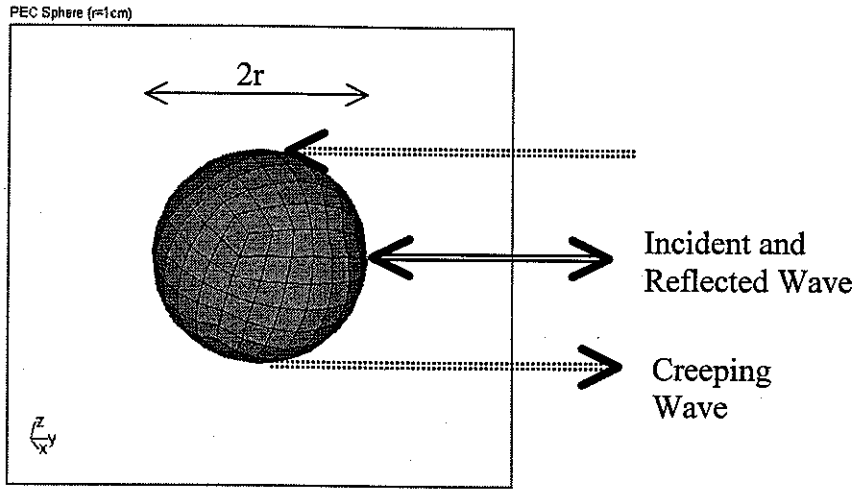

Figure 8. A conducting sphere.

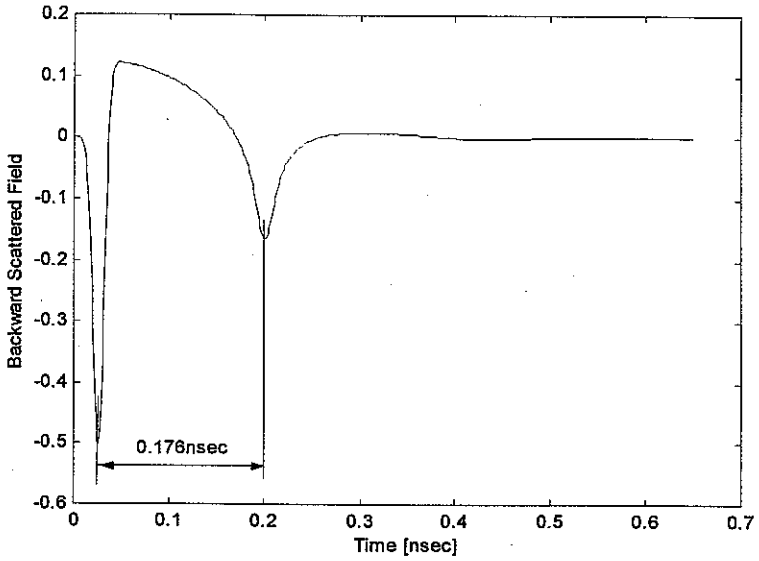

Figure 9. Backward scattered field in the time domain for a conducting sphere.

Pole extractions and approximations with the two methods are done with the entire time domain impulse response. Figure 10 shows that the RMS error is the same for those three methods and the threshold is satisfied when using 18 damped sinusoids with the threshold of -80dB. But the elapsed CPU time is much different. Average CPU time for the MPM is 1.3983sec, for the SS1 is 2.3284sec and that for SS2 is 34.2365sec. The time for MPM is just 60% of that for the SS1 and 4% of that for the SS2. The plots of the CPU times taken by each method are shown in Figure 11.

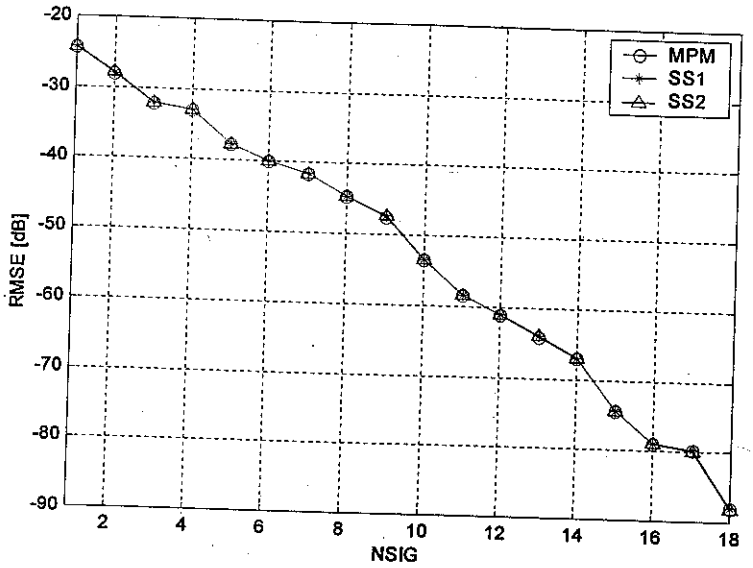

Figure 10. RMS error associated with the reconstructed signal for a conducting sphere.

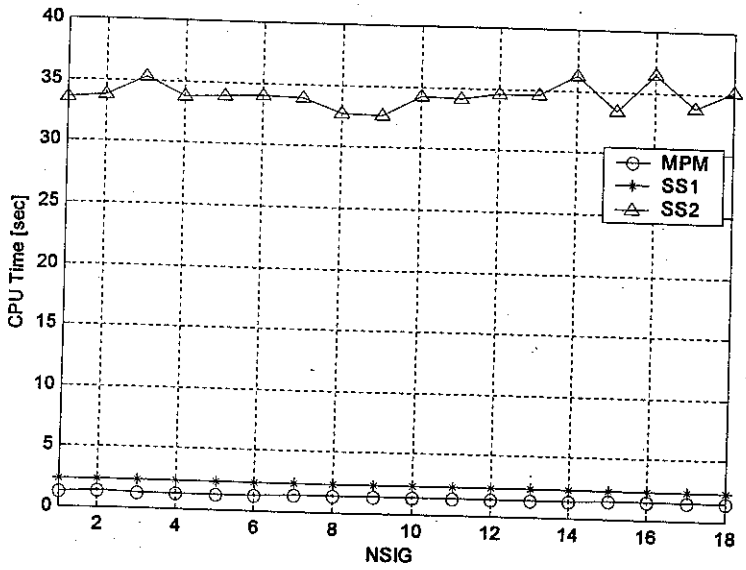

Figure 11. CPU time taken by each method.

Figures 12 and 13 show the extracted complex resonant poles for NSIG (number of damped sinusoid signal) equals 10 and 14. They show that the extracted poles are same for those methods. It means that the singular values are equal even though the starting Hankel matrix for each method is different.

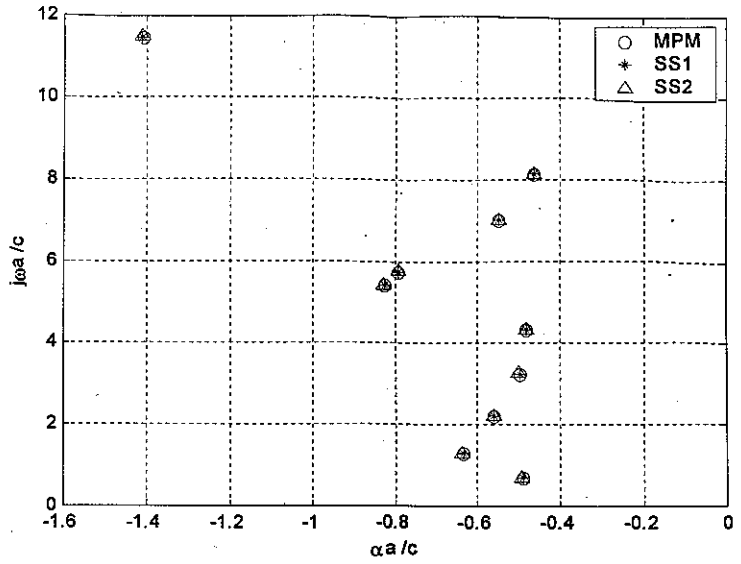

Figure 12. Extracted poles for NSIG = 10 of a conducting sphere.

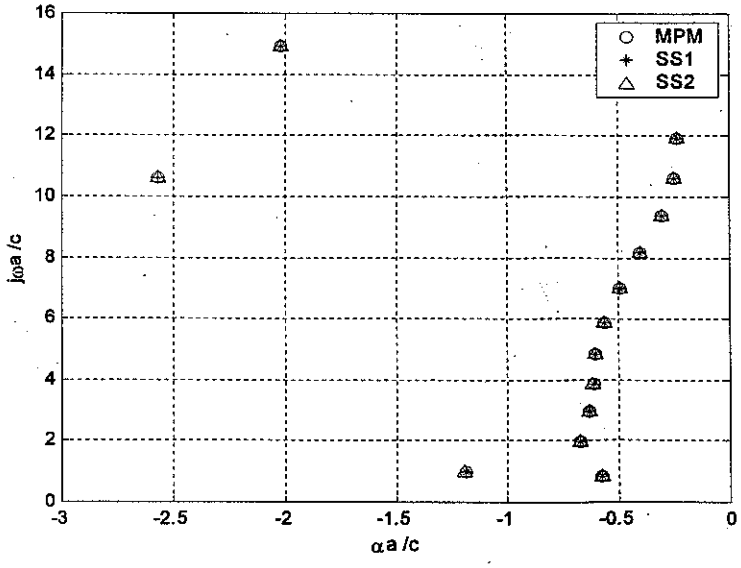

Figure 13. Extracted poles for NSIG = 14 of a conducting sphere.

6.3 Cylinder

For the third example we consider a finite closed cylinder. The length of the cylinder is 1m and its diameter is 0.2m so that the aspect ratio, length/diameter is 5, which is shown in Figure 14. The angle of the incident field is 45 degree from the axis of the cylinder and is θ-polarized. The parameters for the Gaussian window, which is applied to limit the bandwidth of the frequency domain result, are $\sigma = 0.15$ and $ct_0 = 8.5$. After the windowing, the backward scattered field is obtained using the inverse Fourier transform. That is shown in Figure 15.

Pole extractions and approximations with those three methods are done with this time domain signal. Figure 16 shows that the RMS error is the same for all methods and the threshold is satisfied with 15 damped sinusoids. Also the locations of the extracted poles are same for all methods, which is shown in Figure 17.

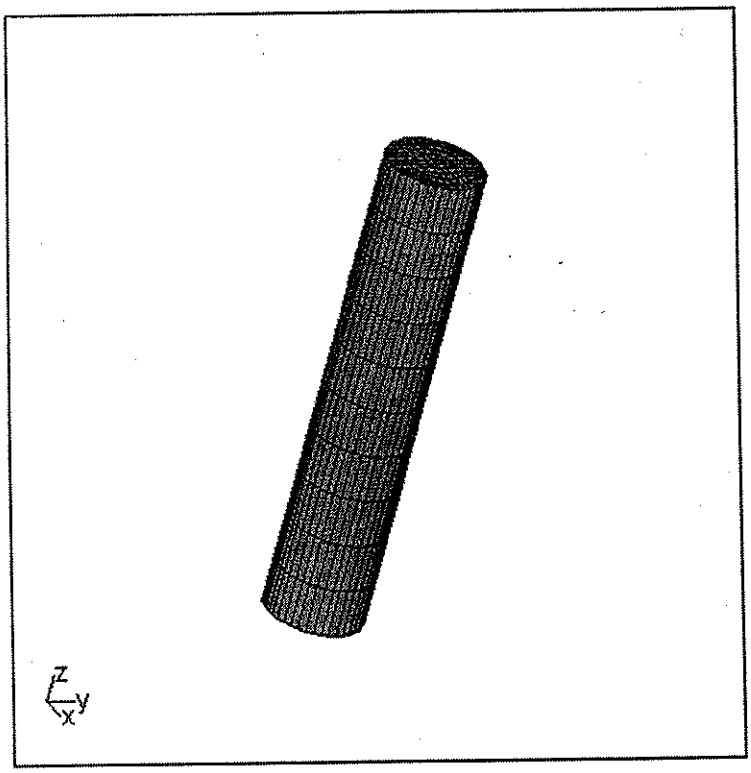

Figure 14. A finite cylinder model with an aspect ratio of L/d = 5.

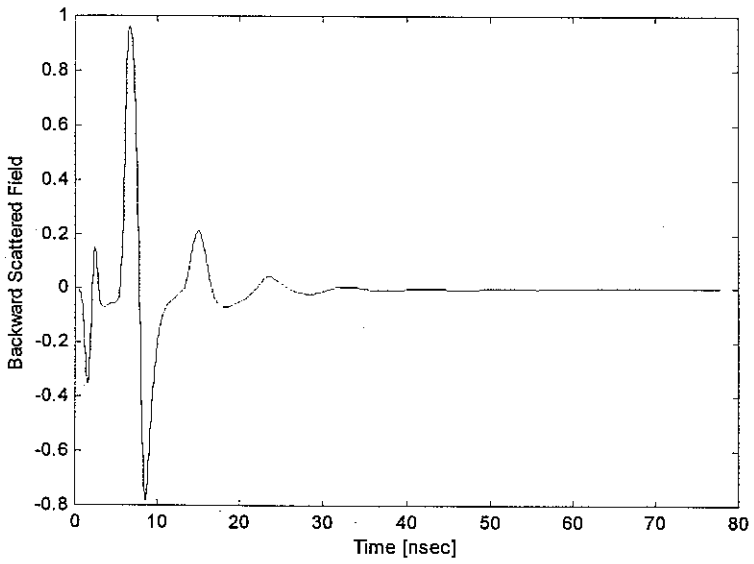

Figure 15. Backward scattered field in the time domain for a finite closed cylinder.

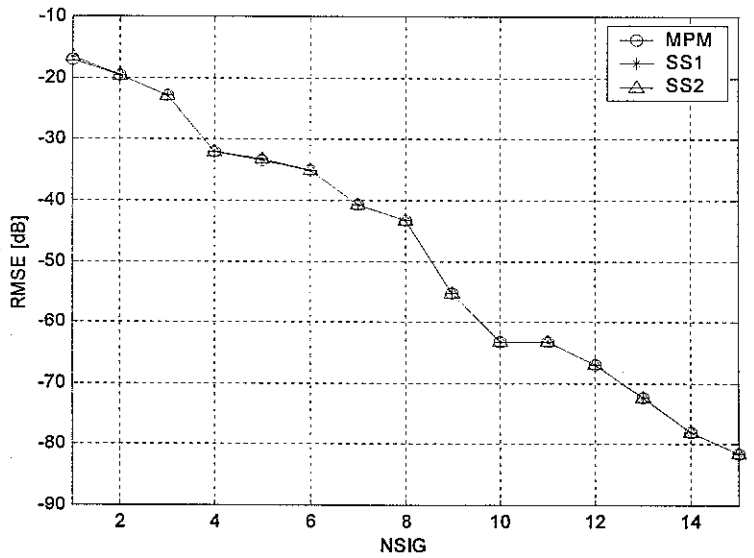

Figure 16. RMS error associated with the reconstructed signal for a finite closed cylinder.

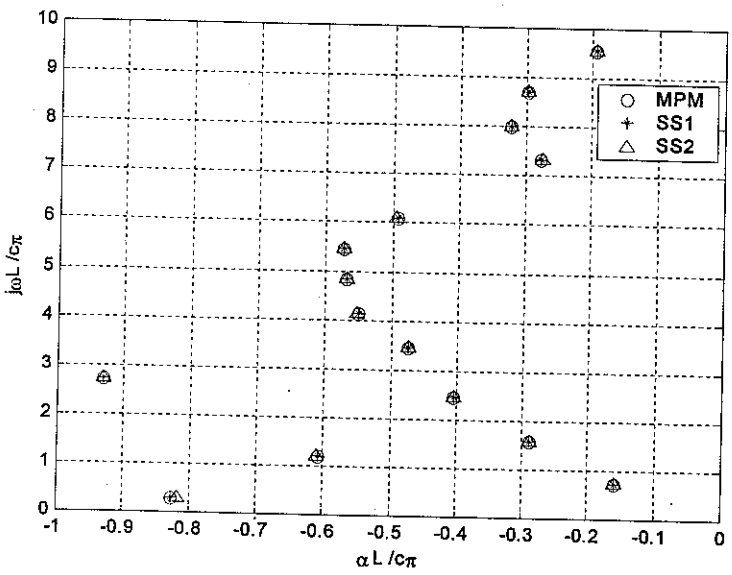

Figure 17. Extracted poles for NSIG = 15 of a finite closed cylinder.

But the elapsed CPU time is much different. Average CPU time for the MPM is 19.0647sec, CPU time for the SS1 is 24.7465 and that for the SS2 is 391.4876sec. The time for the MPM is about 71% of that for SS1 and 4.87% of that for the SS2.

6.4 Dielectric Sphere

The fourth example is chosen to be a dielectric sphere of $\varepsilon_r = 4$ and radius 0.5 m, The backward scattered field has been obtained using WIPL-D in the frequency range of 10-1500MHz. The incident field is coming from the top and is x-polarized. A Gaussian window is applied to limit the bandwidth. The parameters of the Gaussian window are $\sigma = 0.56$ and $ct_0 = 5\sigma$. The inverse transformed time domain data is shown in Figure 18.

Extracted Poles are almost same for all three methods. But there is a little difference for the second state space approach for NSIG = 9 and 10. Figure 19 shows the locations of the poles for NSIG=10. The threshold is satisfied with 10 damped sinusoids for all the methods. That is shown in Figure 20. Average CPU time for the MPM is 18.0860sec, CPU time for the SS1 is 25.7962sec and that for the SS2 is 341.0181sec. The time for the MPM is about 70.11% of that for the SS1 and 5.30% of that for the SS2.

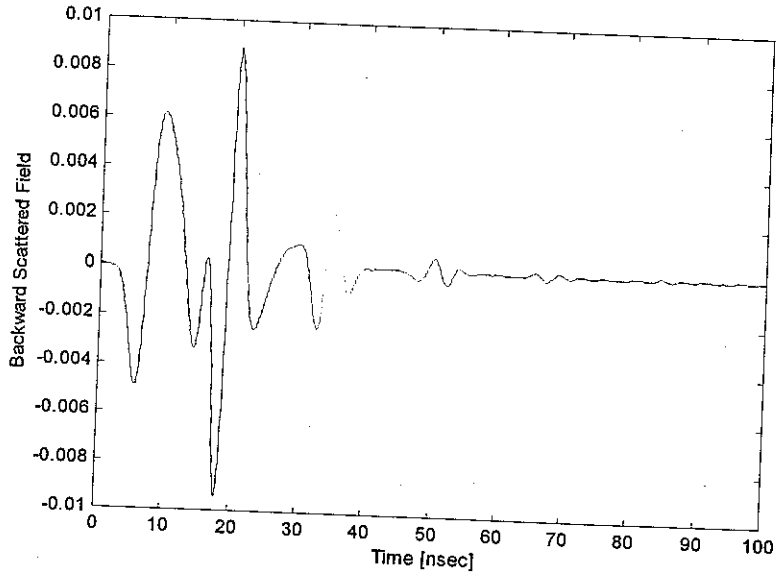

Figure 18. Backward scattered field in the time domain for a dielectric sphere.

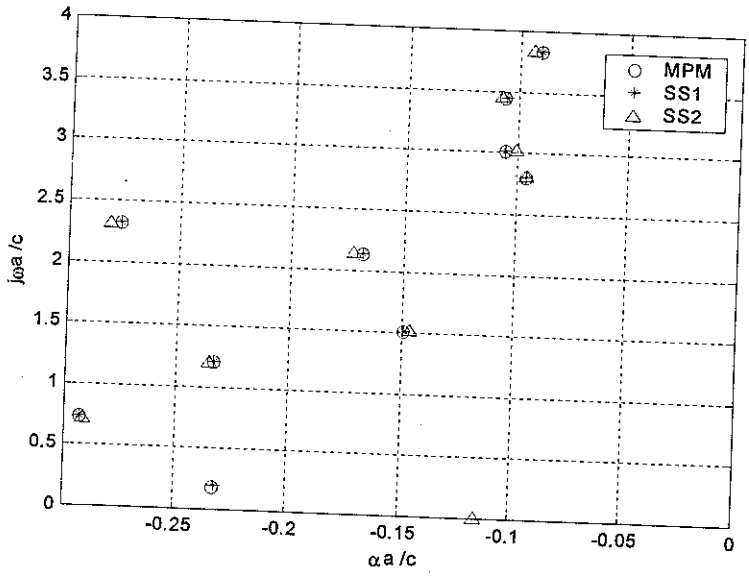

Figure 19. Extracted poles for NSIG = 10 for a dielectric sphere.

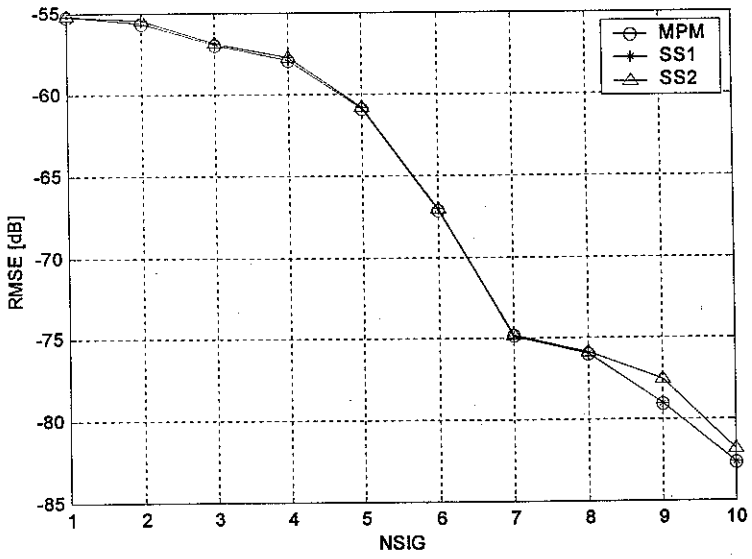

Figure 20. RMS error associated with the reconstructed signal for a dielectric sphere.

6.5 Composite Conducting and a Dielectric Sphere

The last example chosen is a composite sphere of radius 0.5 m, which is shown in Figure 21. Half of it is a perfect conductor and another half is a dielectric with $\varepsilon_r = 4$. The backward scattered field has been obtained using WIPL-D in the frequency range of 10-1500MHz. The incident field is coming from the x-axis and is y-polarized. A Gaussian window is applied to limit the bandwidth. The parameters of the Gaussian window are $\sigma = 0.45$ and $ct_0 = 5.1\sigma$. The inverse transformed time domain data is shown in Figure 22.

Extracted Poles are same for all the methods and the threshold is satisfied with 9 damped sinusoids. That is shown in Figure 23 and Figure 24. Average CPU time for the MPM is 16.95sec, CPU time for the SS1 is 24.7059sec and that for the SS2 is 338.3066sec. The time for the MPM is about 68.61% of that for the SS1 and 5% of that for the SS2.

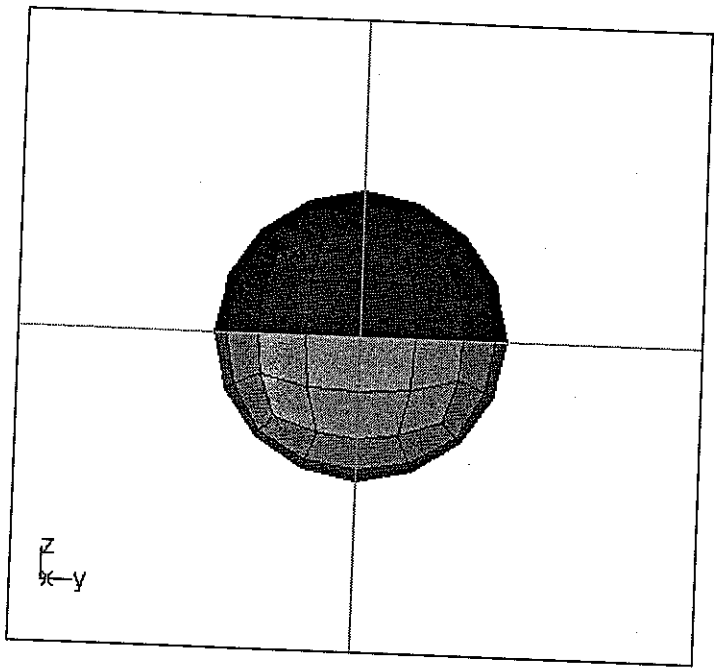

Figure 21. A composite conducting and a dielectric sphere of radius 0.5 m.

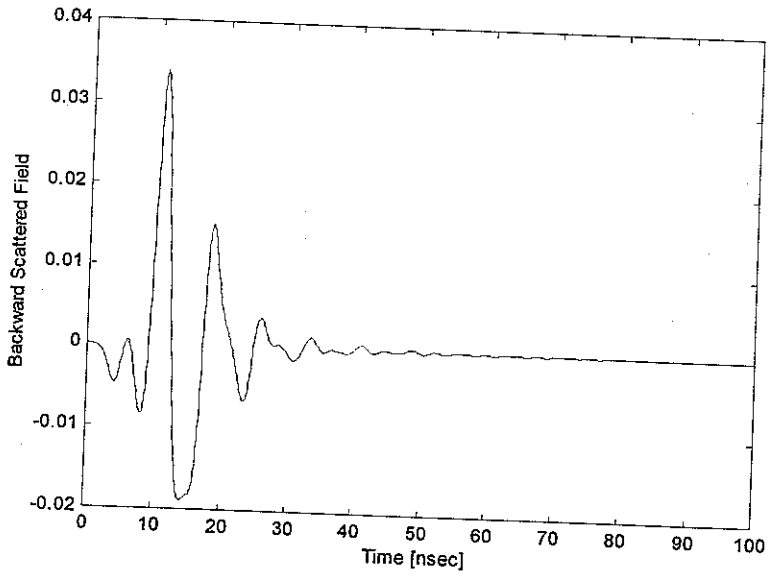

Figure 22. Backward scattered field in the time domain for a composite sphere.

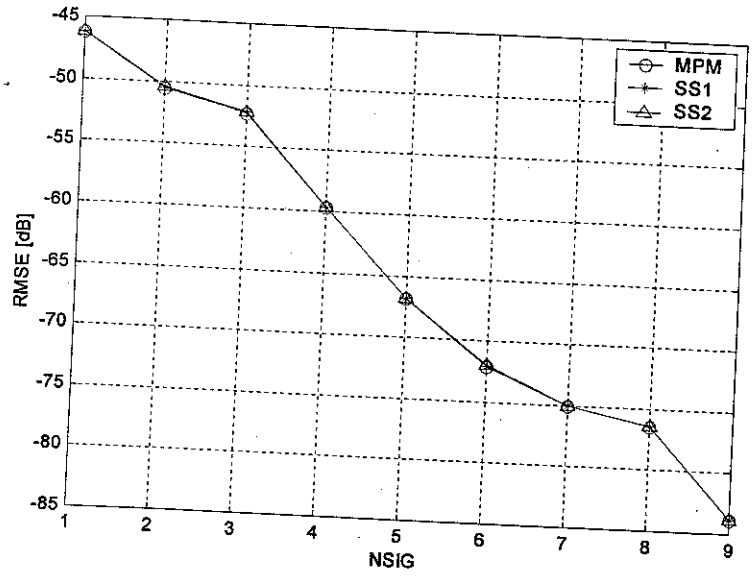

Figure 23. RMS error associated with the reconstructed signal for the composite sphere.

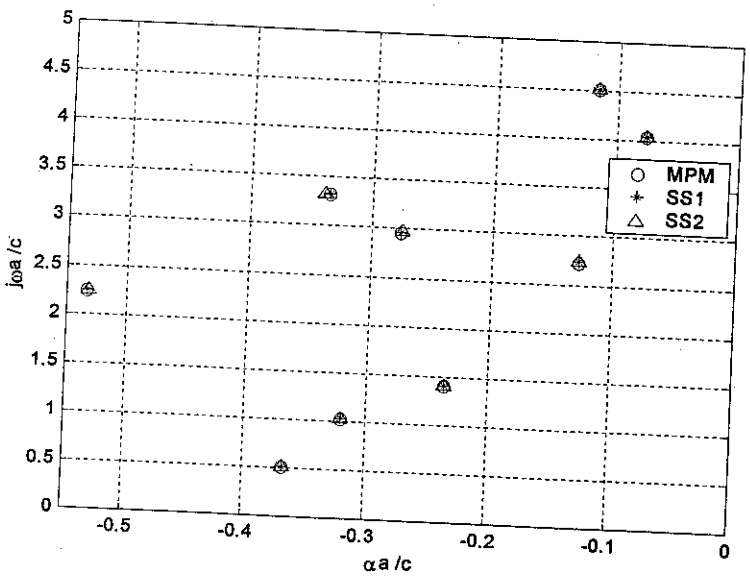

Figure 24. Extracted poles for NSIG = 9 for a composite sphere.

7. Conclusions

Three representative methods for approximating a real function by a sum of complex exponentials have been compared quantitatively. They are generated from three different Hankel matrices and all use a singular value decomposition. The Matrix Pencil Method and the first state space approach display similar results for the extracted poles. But the second state space approach which use extended impulse response Gramian, produce different poles in some cases. The extracted complex poles are same for all the three methods when the data is relatively smooth. But they are different when a signal has pulse-like components (wire case) or is varying rapidly (dielectric sphere). The three methods can perform differently when noise is present in the data, particularly the second state space approach.

There is a big difference in the CPU time for those three methods. Table I provides a summary of the CPU times taken by each model. The CPU time taken by the Matrix Pencil Method is about 60-70% of the CPU time of the first state space approach, and 4-5% of the CPU time of the second State Space approach for comparable accuracy in the results. For the Matrix Pencil Method the original data is used directly but in the second State Space approach using Extended Impulse Response Gramian a multiplication operation is necessary to form each element of the Hankel matrix. There are different versions of the state space method [6], [7] but to calculate the impulse response (Markov parameters) the state space approach with extended impulse response Gramian (EIRG) is used here for comparison.

Table I. Summary of the average CPU time taken by each method.

Model	MPM [sec]	SS1 [sec]	SS2 [sec]	MPM/SS1[%]	MPM/SS2[%]
Wire	11.4489	16.8239	224.8235	68.05	5.09
Sphere	1.3983	2.3284	34.2365	60.05	4.08
Cylinder	19.0647	24.7465	391.4876	71.28	4.87
Di-Sphere	18.0860	25.7962	341.0181	70.11	5.30
Composite Sphere	16.9500	24.7059	338.3066	68.61	5.01

8. References

[1] Y. Hua and T. K. Sarkar, "On SVD for Estimating Generalized Eigenvalues of Singular Matrix Pencil In Noise," *IEEE Trans. On Signal Processing*, Vol. 39, No. 4, pp. 892-900, 1991.

[2] B. D. Rao, "Relation between Matrix Pencil and State Space Based Harmonic Retrieval Methods," *IEEE Trans. On Acoustics, Speech, and Signal Procssing*, Vol. 38, No. 1, pp. 177-179, 1990.

[3] S. Y. Kung, "A New Identification and Model Reduction Algorithm via Singular Value Decompositions," *Proc.Twelth Asilomar Conf. on Circuits, Systems and Computers.*, pp. 705-714, November 6-8, 1978.

[4] T. K. Sarkar and O. Pereira, "Using the Matrix Pencil Method to Estimate the Parameters of a Sum of Complex Exponentials," *IEEE Antennas and Propagation Magazine*, Vol. 37, No. 1, pp. 48-55, 1995.

[5] E-J Ang, V. Sreeram and W. Q. Liu, "Identification/Reduction to a Balanced Realization via the Extended Impulse Response Gramian," *IEEE Trans. On Automatic Control*, Vol. 40, No. 12, pp. 2153-2158.

[6] P. Agathoklis and V. Sreeram, "Identification and Model Reduction from impulse Response data," *Int. J. System Science*, Vol. 21, No. 8, pp. 1541-1552, 1990.

[7] V. Sreeram and P. Agathoklis, "On the Computation of the Gram Matrix in Time Domain and its Application," *IEEE Trans on AutomaticControl*, Vol. AC-38, No. 10, pp. 1516-1520, 1993.

[8] Y. Hua and T. K. Sarkar, "Matrix pencil method for estimating parameters of exponentially damped/undamped sinusoids in noise", *IEEE Trans on Acoustics, Speech, and Signal Processing*, Vol. 38, No. 5, pp. 814-824,1990.

[9] Y. Hua and T. K. Sarkar, "Perturbation Analysis of the TK method for extracting the poles of an electromagnetic system from its transient response", *IEEE Trans on Acoustics, Speech, and Signal Processing*, Vol. 36, No. 2, pp. 228-240, 1988.

[10] B. M. Kolundzija, J. S. Ognjanovic and T. K. Sarkar, "*WIPL-D* (for Windows manual)", Artech House, Norwood, Mass., 2000.

[11] W. Lee, *Transient Scattering from Arbitrarily Shaped Composite Conducting and Dielectric Structures*, Ph. D. Dissertation, Syracuse University, 2001.